Received: 14 April 2020 | Accepted: 17 June 2020
DOI: 10.1002/pros.24039

ORIGINAL ARTICLE

The Prostate WILEY

# Patterns of stemness-associated markers in the development of castration-resistant prostate cancer

Joël R. Federer-Gsponer MD[1] | David C. Müller MD[1] | Tobias Zellweger MD[2] | Maurice Eggimann[3] | Katharina Marston MD[3] | Christian Ruiz PhD[3] | Hans-Helge Seifert MD[1] | Cyrill A. Rentsch MD, PhD[1] | Lukas Bubendorf MD[3] | Clémentine Le Magnen PhD[1,3]

[1]Department of Urology, University Hospital Basel, Basel, Switzerland

[2]Department of Urology, St Clara Hospital, Basel, Switzerland

[3]Institute of Medical Genetics and Pathology, University Hospital Basel, University of Basel, Basel, Switzerland

**Correspondence**
Clémentine Le Magnen, PhD, Institute of Medical Genetics and Pathology, University Hospital Basel, University of Basel, Schönbeinstrasse 40, 4056 Basel, Switzerland.
Email: Clementine.lemagnen@usb.ch

**Funding information**
Fond'Action contre le cancer; Universität Basel, Grant/Award Number: 3MS1025

## Abstract

**Background:** Putative castration-resistant (CR) stem-like cells (CRSC) have been identified based on their ability to initiate and drive prostate cancer (PCa) recurrence following castration in vivo. Yet the relevance of these CRSC in the course of the human disease and particularly for the transition from hormone-naive (HN) to castration-resistance is unclear. In this study, we aimed at deciphering the significance of CRSC markers in PCa progression.

**Methods:** We constructed a tissue microarray comprising 112 matched HN and CR tissue specimens derived from 55 PCa patients. Expression of eight stemness-associated markers (ALDH1A1, ALDH1A3, ALDH3A1, BMI1, NANOG, NKX3.1, OCT4, SOX2) was assessed by immunohistochemistry and scored as a percentage of positive tumor cells. For each marker, the resulting scores were statistically analyzed and compared to pathological and clinical data associated with the samples. Unsupervised clustering analysis was performed to stratify patients according to the expression of the eight CRSC markers. Publicly-available transcriptional datasets comprising HN and CR PCa samples were interrogated to assess the expression of the factors in silico.

**Results:** Immunohistochemical assessment of paired samples revealed atypical patterns of expression and intra- and intertumor heterogeneity for a subset of CRSC markers. While the expression of particular CRSC markers was dynamic over time in some patients, none of the markers showed significant changes in expression upon the development of castration resistance (CR vs HN). Using unsupervised clustering approaches, we identified phenotypic subtypes based on the expression of specific stem-associated markers. In particular, we found (a) patterns of mutual exclusivity for ALDH1A1 and ALDH1A3 expression, which was also observed at the transcriptomic level in publicly-available PCa datasets, and (b) a phenotypic cluster associated with more aggressive features. Finally, by comparing HN and CR matched samples, we identified phenotypic cluster switches (ie, change of phenotypic cluster between the HN and CR state), that may be associated with clinical and predictive relevance.

  

**Conclusions:** Our findings indicate stemness-associated patterns that are associated with the development of castration-resistance. These results pave the way toward a deeper understanding of the relevance of CRSC markers in PCa progression and resistance to androgen-deprivation therapy.

**KEYWORDS**
cancer stem cell, castration-resistant, hormone-naïve, matched samples, prostate cancer

## 1 | INTRODUCTION

Prostate cancer (PCa) remains the most diagnosed cancer type and a leading cause of cancer-related deaths in European men.[1,2] Androgen-deprivation therapy (ADT) is a mainstay of treatment for advanced PCa. While it is initially effective, most tumors eventually become resistant and the emergence of a more aggressive disease referred to as castration-resistant (CR) prostate cancer (CRPC) occurs.[3] Resistance to ADT (ie, castration-resistance) may be driven by small populations of cells endowed with stem-like properties and referred to as cancer stem cells (CSC).[4,5] CSC pools are thought to be resistant to therapy, to drive cancer relapse after treatment, and may expand during tumor development as suggested by the presence of higher CSC contents and the enrichment of stem cell signatures in aggressive tumors and posttreatment settings.[6-8] Despite intense investigation, the origin and the phenotype of CSC remain unresolved in many solid tumors. In particular, it is still unclear whether these cells derive from normal adult stem cells or may arise de novo from non-stem differentiated cells, which have acquired plasticity.[9] CSC may, therefore, be present at the time of diagnosis or arise as a result of treatment-induced plasticity of differentiated tumor cells.[10]

In the prostate, various cell populations have been identified, based on their ability to initiate and drive tissue regeneration and tumor recurrence following ADT in distinct experimental systems. In particular, a population of luminal cells expressing NKX3.1 survives castration and drives tumor reinitiation in mouse and xenograft models.[11,12] These cells, referred to as CARNs (CR NKX3.1 expressing), are endowed with stem-like properties and express stem-associated markers such as NANOG, SOX2, OCT4, and ALDH1A1 in a human established xenograft model.[12] In addition, lineage tracing in vivo enabled the identification of CR populations based on the expression of Bmi1 and/or Sox2[13,14]; notably, these cells are distinct from CARNs, suggesting the coexistence of several CR stem-like cell (CRSC) populations in mouse models. Finally, CSC may be characterized by high activity of the aldehyde dehydrogenase enzyme (ALDH), which occurs via the (co)-action of specific ALDH isoforms.[15-17] While it is likely that distinct subsets of CRSC coexist, it is also possible that the functional relevance of specific subsets may be model- and context-dependent. Considering the difficulties to access relevant samples and perform longitudinal analyses in humans, the relevance of these cell populations for the development of castration-resistance in PCa patients is poorly understood.

In this study, we investigated the expression and clinical significance of a panel of putative CRSC markers, including ALDH1A1, ALDH1A3, ALDH3A1, NANOG, OCT4, SOX2, BMI1, and NKX3.1, in matched specimens derived from patients pre-ADT (hormone-naive [HN] status) and post-ADT (CR status). We observed that expression of particular CRSC markers is heterogeneous and may be dynamic over time within the same patients, but none of the investigated markers showed significant changes in expression upon the development of castration resistance (CR vs HN). Furthermore, we uncovered correlation patterns between markers at the protein level, some of which were also observed in silico in transcriptomic datasets. Finally, we identified CRSC-associated phenotypic subtypes based on the tissue microarray (TMA) immunostaining data that (a) highlighted patterns of mutual exclusivity for ALDH1A1 and ALDH1A3 expression and (b) may be associated with clinical and predictive relevance in PCa.

## 2 | MATERIAL AND METHODS

### 2.1 | Patients and tissue samples

All PCa samples were obtained under an approval by the Ethics Committee of Northwestern and Central Switzerland (EKNZ, No EK/1311 and 2015/228). Tumor-free prostate core needle biopsies were used for the analysis of benign prostate (n = 3 patients). PCa biopsies included in the TMA were taken during routine clinical treatment. Samples were selected based on the following inclusion criteria: (a) histologically-diagnosed PCa, (b) tumor-containing biopsies available at HN and CR state, and (c) sufficient quality and amount of material, as evaluated by experienced pathologists (LB and KM). Castration-resistance was defined as either biochemical progression (ie, serum PSA progression according to *Prostate Cancer Clinical Trials Working Group* criteria[18]) or clinical progression (ie, growth of metastasis in size or number or local progression to the point of need for surgical intervention). A TMA comprising 112 matched HN/CR tissues specimens, and including 107 transurethral resections and five distant metastases derived from 55 PCa patients was constructed as previously described.[19] Briefly, tissue cylinders with a diameter of 1 mm were punched from the patient's tissue blocks containing the specimens using the robotic precision instrument Grand Master TMA (3D Histech). Clinical and pathological characteristics of the patients included in the TMA are described in Table S1.

## 2.2 | Immunohistochemistry

Immunohistochemical analyses were conducted according to standard indirect immunoperoxidase procedures as previously reported.[20] Expression of the eight CRSC markers, Chromogranin A, and Ki67 was assessed using heat-mediated antigen retrieval before the staining with the following antibodies and dilutions: ALDH1A1 (1:50; ab52492; Abcam), ALDH1A3 (1:25; HPA046271; Atlas Antibodies), ALDH3A1 (1:50; SP298; Spring Bioscience antibody), NKX3.1 (Ventana 760-5086, ready to use), BMI1 (1:50; HPA030472; ATLAS), OCT4 (Ventana 760-4392, ready to use) NANOG (1:200; ab109250; Abcam), SOX2 (Ventana 760-4621, ready to use) Chromogranin A (Ventana 760-2519, ready to use), and Ki67 (Mib1, Dako IR626, ready to use). To ensure antibody specificity and sensitivity, antibodies were tested on appropriate positive controls (as shown in Figure S1).

## 2.3 | TMA analysis

The staining was blindly scored by an experienced pathologist as a percentage of positive tumor cells for ALDH1A1, ALDH1A3, ALDH3A1, NKX3.1, BMI1, OCT4, NANOG, SOX2, Ki67, and Chromogranin A. A score greater than 0 was considered positive. Two independent cores for each specimen were scored and the highest value was considered for analysis.

## 2.4 | Computational analyses

For analyses of gene expression levels in published datasets, messenger RNA expression (*z* scores), and clinical data were exported from cBioPortal.[21,22] Analyses were performed on two datasets comprised of untreated primary PCa samples[23,24] and two datasets comprised of advanced CRPC samples.[25,26] Unsupervised clustering (k-nearest neighbors with 100 repetitions) of the TMA protein expression data was performed using R (version 3.5.3)[27] and the cluster number of 4 was determined by biological reasoning on the cluster composition and compared to the computed elbow point. For clustering, missing values in the TMA data were imputed using multiple chained imputation by predictive mean matching as provided by the "MICE" package[28]; samples with information missing for more than four markers were excluded from imputation and clustering. Cluster computation and visualization were done using the "Complex Heatmap" package[29] and Pearson's coefficient was used as the distance metrics.

## 2.5 | Statistical analyses

All statistical analyses were performed using R (version 3.5.3). Expression levels of markers before and post-ADT were compared using unpaired and paired Wilcox rank-sum tests. Time to castration resistance was analyzed in a univariate fashion using the logrank test and in a multivariate fashion considering all analyzed markers together by fitting a Cox proportional hazard model as implemented in the "survival" package.[30] Associations between markers expression and clinical parameters (T and N stages at diagnosis, PSA at diagnosis) were assessed using rank-based tests (Kruskal-Wallis test, Spearman correlation). Mutual exclusivity analysis on the TMA data was done using the odds ratio and the Fisher exact test and time to castration resistance was compared using a logrank test after dichotomizing the groups into negative and positive for IHC marker staining. Similarly, public datasets were dichotomized at the median and compared using the odds ratio and the Fisher exact test. Two-sided *P* values were calculated, as done previously.[31] All pairwise correlations were done using Spearman's correlation ($r_s$) and the Spearman's rank test for the non-normally distributed TMA data. For published datasets, Pearson's correlation method ($r_p$) was used.

# 3 | RESULTS

## 3.1 | Inter- and intratumor heterogeneity of putative CRSC markers in PCa

To determine their patterns of expression in the normal setting, we analyzed the expression of eight putative CRSC markers in representative benign prostatic tissues (n = 3 patients). As expected, the Homeobox protein NKX3.1 was highly expressed in prostate epithelial cells and the Polycomb complex protein BMI1 was abundantly expressed in epithelial and stromal cells (Figure 1A,B, left panels). Expression of the pluripotency-associated factor OCT4 was observed in the cytoplasm of rare cells exhibiting a neuroendocrine-like morphology in all tested samples (Figure 1C and Figure S2A, left panels). In contrast, all benign samples were negative for the other pluripotency-associated factor NANOG (Figure 1D, left panel). Positivity for SOX2 and the ALDH-specific isoforms ALDH3A1 and ALDH1A1 was restricted to subsets of basal cells, while ALDH1A3 expression was mainly observed in luminal cells of the benign prostate (Figure 1E-H and Figure S2B-D, left panels).

To assess the prognostic and clinical relevance of the putative CRSC markers in PCa, we constructed a TMA comprising 112 matched HN and CR tissues specimens, associated with detailed pathological and clinical data. Similar to benign specimens, expression of NKX3.1 and BMI1 was generally high in all tested PCa samples (96.8% positive [91/94], average score: 96.0 for NKX3.1, and 94.7% positive [90/95], average score: 95.0 for BMI1, Figure 1A,B right panels and Table S2). In contrast to these markers, positivity for the pluripotency-associated factors OCT4 and NANOG was less frequent and occurred in a lower number of cells (22.2% positive [22/99], average score: 1.9, and 3.1% positive [3/97], average score: 1.2, respectively). In positive PCa samples, OCT4 and NANOG expression was exclusively localized to the cytoplasm, in contrast with the nuclear expression observed in seminoma control samples (Figure 1C,D right panels, Table S2, Figures S1 and S2A). Notably, similar to benign

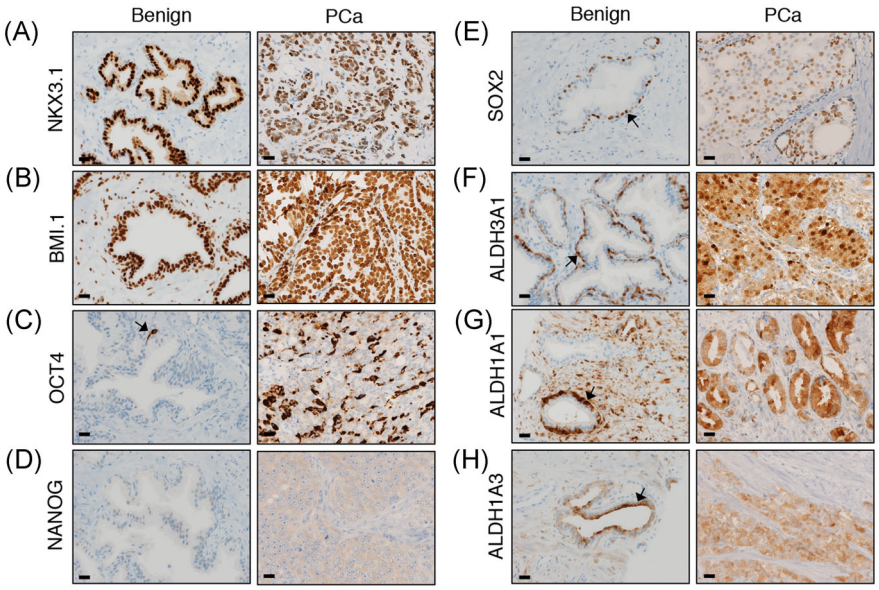


**FIGURE 1** Expression and localization of putative CRSC markers in the benign prostate and in PCa. Representative images of immunohistochemical staining for NKX3.1 (A), BMI1 (B), OCT4 (C), NANOG (D), SOX2 (E), ALDH3A1 (F), ALDH1A1 (G), and ALDH1A3 (H). Arrows indicate expression of OCT4 in rare neuroendocrine-like cells of the benign prostate (C, left panel), expression of SOX2, ALDH3A1, and ALDH1A1 in benign prostate basal cells (E, F, G, left panels), and of ALDH1A3 in benign prostate luminal cells (H, left panel). Scale bars represent 20 μm. ALDH, aldehyde dehydrogenase enzyme; CRSC, castration-resistant stem-like cell; PCa, prostate cancer

specimens, cytoplasmic expression of OCT4 appeared to be restricted to cells with a neuroendocrine morphology in PCa samples (Figure 1C right panel, Figures S2A and S3A). Confirming these observations, expression of the neuroendocrine-associated marker Chromogranin A (CGA) significantly correlated with OCT4 expression (Spearman's rank correlation, $R = .59$, $P = 1.4e\text{-}10$; Figure S3A,B). Similarly, expression of *POU5F1* (ie, the gene encoding OCT4), significantly correlated with that of *CHGA* (ie, the gene encoding Chromogranin A) in a transcriptomic dataset comprising 131 primary PCa samples[24] (Pearson correlation, $R = .48$, $P = 5.8e\text{-}09$; Figure S3B). These findings are in line with previous studies, highlighting the expression of cytoplasmic OCT4 in a subset of neuroendocrine prostate cells.[32,33] Nuclear positivity for SOX2 was detected in 16.1% of PCa samples (15/93; average score: 7.1, Table S2; Figure 1E and Figure S2B right panels). Finally, immunohistochemical staining for the ALDH-specific isoforms ALDH1A1, ALDH1A3, ALDH3A1 revealed heterogeneity between and within samples for the three isoforms with 38.5% (37/96; average score: 19.0), 38.3% (36/94; average score: 24.0), and 3.9% (4/102; average score: 2.0) of positive samples for ALDH1A1, ALDH1A3, and ALDH3A1, respectively (Figure 1F-H, Figure S2C,D right panels, Table S2).

## 3.2 | Progression to castration-resistance is not associated with expression of single CRSC-associated markers

Recent studies have suggested that CSC may be enriched in post-treatment settings in various tumor types including PCa.[6] We, therefore, assessed and compared the expression and the frequency of each CRSC marker in the HN and the CR group. Unpaired statistical analyses revealed similar levels of expression between the HN and CR group for ALDH1A1, ALDH1A3, ALDH3A1, NKX3.1, BMI1, NANOG, and OCT4 ($P$ values ranging from 0.08 to 0.99, two-sided Wilcoxon test, Figure 2A). In contrast, expression of SOX2 was significantly higher in the CR group as compared to the HN group ($P = .04$, two-sided Wilcoxon test, Figure 2A). Given that our TMA comprised matched primary HN and CR samples, we performed paired statistical analyses to directly compare the HN and CR state for each patient. For a subgroup of markers (ie, ALDH1A1, ALDH1A3, SOX2), we observed dynamic changes of expression when comparing HN specimens and their matched CR samples but no significant difference of expression between matched HN and CR samples was found for any of the tested markers ($P$ values ranging from 0.11 to 1, two-sided Wilcoxon test, Figure 2B). Thus, cells expressing these putative CRSC markers do not appear to be significantly enriched in the CR state.

Expression of Ki67 is associated with prognostic and predictive significance in PCa and may identify cell populations with distinct proliferative potential[34,35]; we, therefore, assessed Ki67 expression and its association with that of CRSC markers in the HN and the CR groups. In both paired and unpaired analyses, expression of Ki67 was significantly higher in CR samples as compared to HN samples ($P < .01$, two-sided Wilcoxon test, Figure 2A,B). Expression of Ki67 negatively correlated with expression of BMI1 and NKX3.1 in the CR state but not with that of any other marker in both HN and CR groups (Spearman's rank correlation, $R = -.37$, $P = .025$ and $R = -0.46$, $P = .003$, respectively; Figure S4). We next evaluated whether

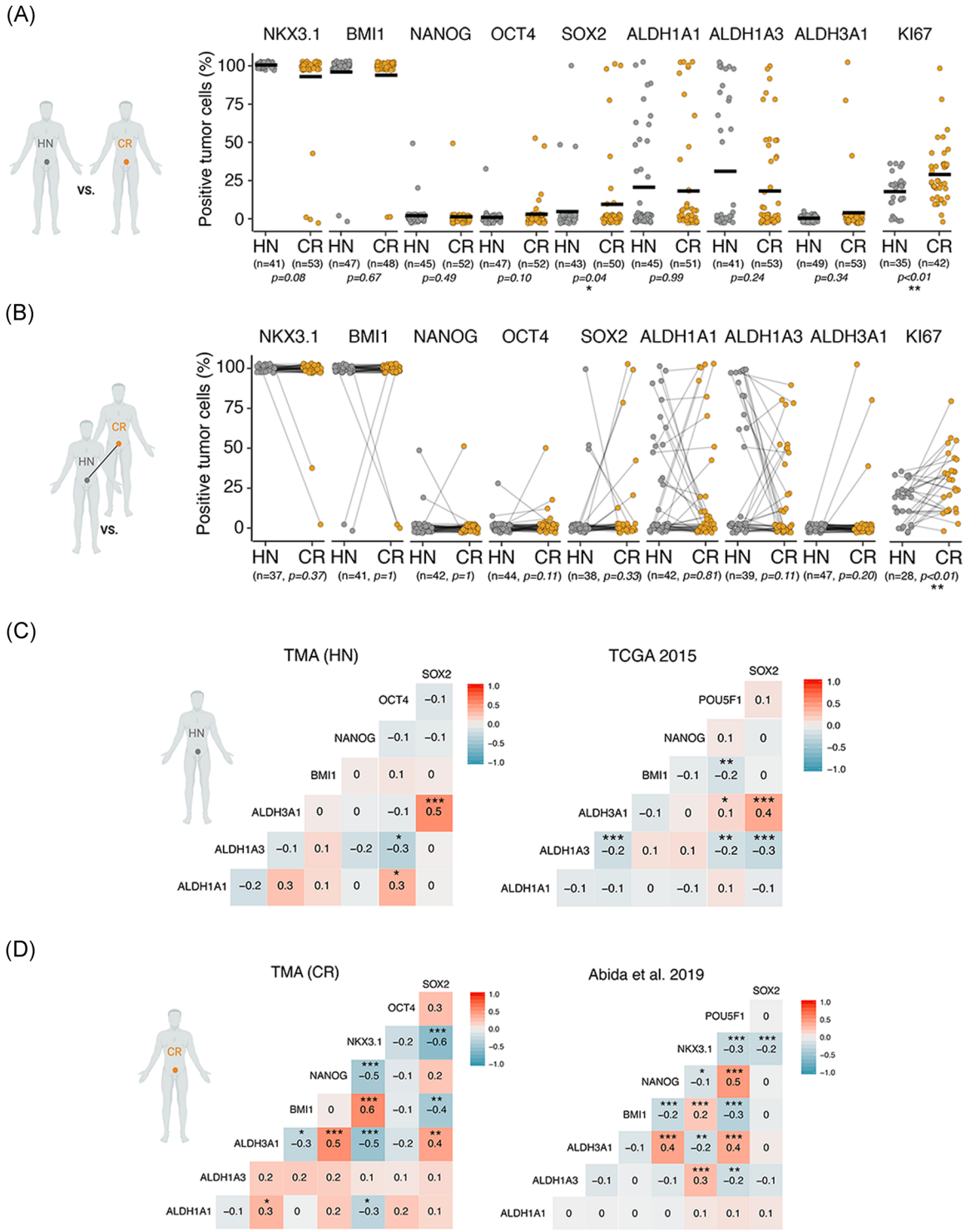


**FIGURE 2** Expression of single CRSC-associated markers in hormone-naive (HN) and castration-resistant (CR) PCa samples. Expression of CRSC markers and Ki67 was specifically scored in tumor cells and compared between all HN and CR samples (A) and between matched HN and CR samples (B) using Wilcoxon analysis. Means (black bars), number of samples, and *P* values are indicated for each marker. (C) Correlation maps of expression for all markers in HN samples as assessed at protein level in the TMA (left) and at transcriptional level in a published dataset comprising 290 untreated PCa samples (right). Note that NKX3.1 was not comprised in the analyses given its ubiquitous expression in all HN samples (D) Correlation maps of expression for all markers in CR samples as assessed at protein level in the TMA (left) and at transcriptional level in a published dataset comprising 212 CRPC samples (right). *P* values (*$P < .05$, **$P < .01$, ***$P < .001$) and $r_s$ are indicated for each combination. Spearman tests and Pearson tests were used for statistical analyses of the TMA immunostaining and transcriptomic datasets, respectively. CRSC, castration-resistant stem-like cell; PCa, prostate cancer

positivity for each single marker was associated with distinct pathological and clinical features. We did not observe any difference in terms of Gleason score, time to castration-resistance, and overall survival for patients exhibiting positivity for single markers in the HN or CR state as compared to patients whose samples were negative ($P > .05$ for all markers, Figure S5-S7). In addition, no significant association was found between CRSC markers expression and other clinical parameters such as T and N stages at diagnosis and PSA levels at diagnosis ($P > .05$, Kruskal-Wallis test, Spearman correlation, Table S3).

### 3.3 | Correlation analyses suggest putative relationships between CRSC-associated markers

To gain insight into putative relationships between CRSC markers in PCa, we performed correlation analysis of expression for each marker combination in HN and CR samples. In HN samples, these analyses revealed a positive correlation of expression between ALDH3A1 and SOX2 ($r_s = .5$, $P < .001$) and between ALDH1A1 and OCT4 ($r_s = .3$, $P = .022$), as well as a negative correlation between ALDH1A3 and OCT4 ($r_s = -0.3$, $P = .034$) (Figure 2C). Given that this type of analysis may be biased by the low number of positive samples for some markers, we complemented them by analyzing gene expression data obtained from a publicly-available dataset comprising "untreated" primary PCa samples (n = 290).[23] In this dataset, significant positive correlation of expression between *ALDH3A1* and *SOX2* ($r_p = .4$, $P < .001$) and negative correlation between *ALDH1A3* and *POU5F1* ($r_p = -.2$, $P = .002$) was also observed (Figure 2C).

In CR TMA samples, we observed positive correlation of expression between ALDH3A1 and NANOG ($r_s = 0.5$, $P < .001$), ALDH3A1 and SOX2 ($r_s = .4$, $P < .01$), ALDH3A1 and ALDH1A1 ($r_s = .3$, $P = .02$), and BMI1 and NKX3.1 ($r_s = 0.6$, $P < .001$). Significant negative correlation of expression included ALDH3A1 and BMI1 ($r_s = -.3$, $P = .045$), ALDH3A1 and NKX3.1 ($r_s = -.5$, $P < .001$), ALDH1A1 and NKX3.1 ($r_s = -.3$, $P = .03$), BMI1 and SOX2 ($r_s = -.4$, $P < .01$), NANOG and NKX3.1 ($r_s = -.5$, $P < .001$), and SOX2 and NKX3.1 ($r_s = -.6$, $P < .001$) (Figure 2D). Similar to our approach for HN samples, we complemented these TMA analyses by examining gene expression profiles obtained from a publicly-available dataset comprising CRPC samples (n = 212).[25] In this dataset, we were able to confirm similar significant correlation patterns between SOX2 and NKX3.1 ($r_p = -.23$, $P < .01$), NANOG and NKX3.1 ($r_p = -.15$, $P = .03$), BMI1 and NKX3.1 ($r_p = .23$, $P < .01$), ALDH3A1 and NANOG ($r_p = 0.43$, $P < .001$), and ALDH3A1 and NKX3.1 ($r_p = -.21$, $P < .01$) (Figure 2D).

### 3.4 | Unsupervised clustering analysis identifies phenotypic subtypes based on the expression of specific CRSC markers

We next evaluated whether combinations of specific markers could identify distinct subsets of patients in our cohort of longitudinal samples. To stratify patients according to the expression of CRSC markers, we performed unsupervised hierarchical cluster analysis of the TMA immunostaining data for HN and CR samples. This strategy led to the separation of the samples in four groups (clusters 1 to 4), which revealed patterns of coexpression or of mutual exclusivity for specific markers (Figure 3A-C). Clusters 1 and 3 were mainly characterized by expression of either one ALDH isoform (cluster 1: $ALDH1A3^{+/High}$, $ALDH1A1^{-/Low}$ and cluster 3: $ALDH1A1^{+/High}$, $ALDH1A3^{-/Low}$), while cluster 2 mainly comprised samples with low or no expression of both ALDH1A3 and ALDH1A1 (Figure 3A,B and Figure S8A). Cluster 4 represented a minor group (n = 3) exclusively comprising CRPC samples characterized by high expression of SOX2 and negativity for NKX3.1 (Figure 3A,B and Figure S8A).

As suggested by the cluster analysis, expression of ALDH1A1 and ALDH1A3 was mutually exclusive (odds ratio = 0.226, $P < .01$, Fisher's exact test, Figure 3C). This pattern of mutually exclusive expression was also observed at transcriptomic level across several datasets[23-25] (Figure S8B).

### 3.5 | CRSC-associated phenotypic clusters may have clinical and predictive relevance

Aggressive variants of cancer have been shown to display characteristics of poorly differentiated tissues and to express molecular signatures of stem cells.[8] We, therefore, assessed whether the distinct clusters were enriched in subsets of patients with aggressive clinical and/or pathological features. Each sample was assigned a histological type and was either classified as classical adenocarcinoma ("acinar/solid") or as neuroendocrine prostate cancer (NEPC), an aggressive variant of PCa associated with adverse prognosis[36] (Figure 3A). In addition, a subset of adenocarcinoma samples was associated with cribriform features, a tumor growth pattern which correlates with poor clinical outcome.[37] These features were observed in 11/94 samples included in the clustering analysis and were distributed without evident enrichment in one cluster type ("cribriform", Figure 3A). Noteworthy, out of three samples positive for SOX2 in the HN group, two exhibited cribriform features. Finally, cluster 4 was exclusively represented by cases of CR-NEPC, which were highly positive for SOX2 (n = 3/3) and expressed OCT4 (n = 2/3). To determine whether proliferation levels were different between distinct clusters, we allocated each sample to its respective Ki67 level (Figure 3A). While cluster 4-CR samples clearly exhibited high Ki67, the number of samples was too low (n = 3) and no significant difference was found in terms of Ki67 expression between CRSC-associated clusters (Wilcoxon rank-sum test, $P > .05$; Figure 3A and Figure S8A).

We next evaluated whether CRSC-associated clusters were associated with particular clinical features, by comparing pathological and clinical data for each patients' group. While no difference was found in terms of Gleason score, cluster 2-HN samples were associated with shorter time to castration-resistance as compared to those with clusters 1 and 3 ($P < .0001$, logrank test; Figure 3D and

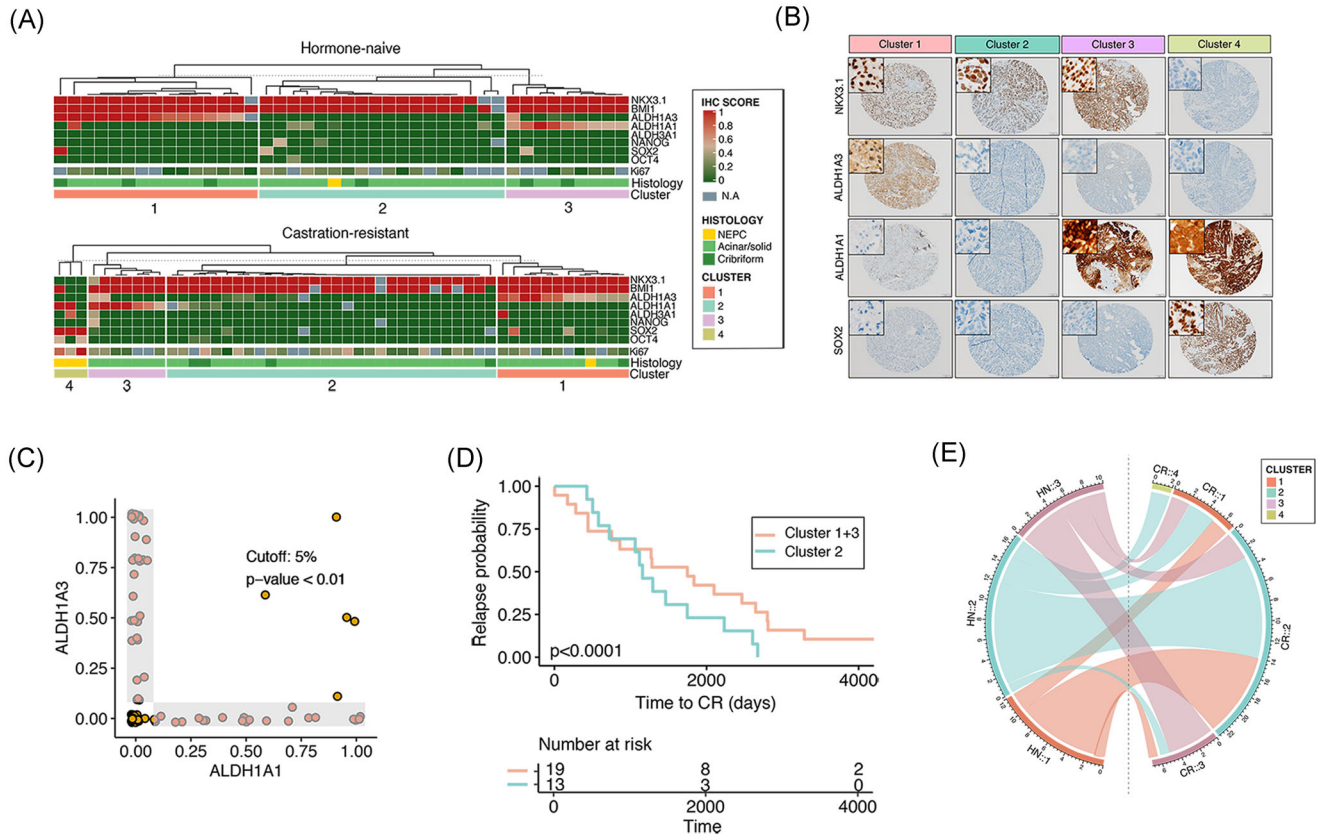


**FIGURE 3** Unsupervised clustering analysis identifies phenotypic subtypes based on the expression of specific CRSC markers with potential clinical relevance. A, Unsupervised k-means clustering analysis identifies CRSC-related phenotypic subtypes (k = 4). Expression of Ki67 as assessed by IHC is shown for each individual sample. Color code for IHC score, histological subtype, and cluster number are indicated in the legend. N.A.: not available. B, Representative images of immunohistochemical staining for NKX3.1, ALDH1A3, ALDH1A1, and SOX2 in PCa samples with phenotypic clusters 1 to 4. Scale bars represent 100 μm. C, Scatter plot showing expression of ALDH1A1 and ALDH1A3 in the HN/CR TMA. D, Survival analysis comparing patients with cluster 2 and patients with clusters 1 and 3 in the HN group ($P < .0001$, logrank test) (E) Chord diagram depicting phenotypic clusters dynamic between CR and HN paired samples. Chords exemplify the number of patients switching cluster upon development of CR. CRSC, castration-resistant stem-like cell; PCa, prostate cancer

Figure S8C). In addition, by comparing matched HN and CR samples, we identified phenotypic cluster switches (ie, change of phenotypic cluster between the HN and CR state), suggesting that CRSC-associated phenotypes are dynamic between HN and CR states (Figure 3E). Notably, cluster 4-CR samples, which are associated with an NEPC histology and aggressive features, exclusively derived from cluster 2-HN samples (ALDH1A1/ALDH1A3$^{-/Low}$).

## 4 | DISCUSSION

In this study, we have investigated the expression of eight stem-associated markers that are functionally relevant for castration-resistance in vivo. By analyzing matched HN and CR resections, we provide insight into the dynamic of expression of these CRSC markers in the path toward castration-resistance. While a group of markers showed heterogeneous and dynamic expression (ALDH1A1, ALDH1A3, SOX2), others were expressed at a high level irrespectively of the castration state (NKX3.1, BMI1) (Figures 1-2 and Table S2). High expression of these markers across samples may be explained by their multifaceted role in prostate stemness and differentiation; as an example, while NKX3.1 marks and is necessary for the maintenance of a population of prostate stem cells, it also controls a transcriptional network driving luminal differentiation and is commonly expressed by a majority of non-stem prostate cells.[11,38] In contrast, the pluripotency factors OCT4 and NANOG and the ALDH3A1 isoform were expressed in a limited subset of patients. In particular, we observed atypical subcellular localization of OCT4 and NANOG in the cytoplasm of PCa cells, which may provide insight into their putative role in PCa.[39] In agreement with previous studies, OCT4 expression was restricted to a subset of Chromogranin A positive neuroendocrine cells, suggesting a possible association between OCT4 and neuroendocrine differentiation[32,33] (Figure S3).

When comparing the expression of single markers in matched HN and CR samples, no significant difference was found, suggesting that these particular CRSC markers are not enriched in the post-ADT setting

(Figure 2). Correlation analysis of marker expression in HN and CR samples highlighted putative relationships between CRSC markers in our TMA and transcriptomic data in silico (Figure 2). Differences in terms of the correlation between datasets may be accounted by distinct sample cohorts (metastasis vs prostate resections) and the type of analyses (protein vs transcriptional). Despite these differences, common association patterns between markers (eg, ALDH3A1 and SOX2) were identified in both our TMA and published datasets, which warrants further investigation in larger cohorts of samples.

Given that CRSC may be defined by combinations of markers, we stratified HN and CR samples according to the expression of the eight CRSC markers using unsupervised clustering analysis. Strikingly, three similar cluster groups (clusters 1-3) were identified in the HN and CR group, which appeared to be mainly driven by the expression of ALDH1A1 and/or ALDH1A3 and highlighted frequent mutual exclusivity between both markers (Figure 3 and figure S8A,B). This pattern of expression is particularly intriguing considering that these distinct ALDH isoforms represent functional regulators of stem cells and may have differential roles in mediating cancer initiation and progression, as well as treatment resistance.[40,41] Finally, the fourth cluster was exclusively represented by histologically-distinct cases of CR-NEPC samples characterized by negativity for NKX3.1 and high expression of SOX2, consistent with its role in promoting neuroendocrine differentiation upon ADT.[42] Thus, whereas samples with a cluster 4 phenotype may be easily identified by their clear neuroendocrine histology, assessing the expression of ALDH1A1 and ALDH1A3 may be sufficient to distinguish morphologically-similar clusters 1 to 3 in future validation studies.

While the expression of single markers did not associate with particular clinical features, CRSC-associated clusters may provide insight into the aggressiveness of the tumors. In particular, at HN state, patients with a cluster 2 PCa (ie, negative/low expression of both ALDH1A1 and ALDH1A3) exhibited a shorter time to castration-resistance as compared to patients with clusters 1 and 3 PCa (ie, positivity for at least one isoform). Moreover, by tracking the dynamics of CRSC-associated clusters between matched HN/CR samples, we found that CRPC with a phenotypic cluster 4 and an NEPC histology that typically associate with aggressive features and poorer prognosis, exclusively derive from HN-cluster 2 samples. Altogether, these data suggest that phenotypic dynamics may be patient-specific and support the clinical relevance of CRSC-associated phenotypic clusters.

Our study may be hampered by several limitations that are inherent with the type of samples used in this study. First, as we investigated only two cores for each sample, our analyses may fail fully capturing intratumor heterogeneity, a phenomenon which is frequently observed in PCa.[43] While we cannot completely overcome this limitation, we have reduced it by selecting the most representative tumor areas for each patients' sample following detailed histological assessment. In addition, the limited number of samples included in our cohort (n = 112 HN and CR PCa) prevented us from drawing more definitive conclusions regarding the prognostic and predictive value of the CRSC markers. Yet, the rarity of our samples' cohort (ie, matched HN and CR prostate resections) provided a unique insight into the relevance of these markers for castration resistance in the context of the native prostate microenvironment. Finally, the expression of stemness-associated markers may be highly dynamic, dependent upon cellular plasticity, and there may be consequently no stable phenotype as reported for other tumor types.[9,44] Our investigations may, therefore, be biased by the time point for sampling, which is highly dependent upon clinical requirements.

Nevertheless, our analyses allowed elucidating cellular localization and expression of specific markers in longitudinal pre- and post-ADT samples and uncovering dynamics between markers that may be missed in transcriptional analyses of bulk tissue. In particular, deciphering the relationship between ALDH1A1 and ALDH1A3 and whether they differentially contribute to PCa progression warrants further investigation. In addition, our analyses highlight the utility of performing more comprehensive analyses incorporating additional putative CRSC markers (eg, Ly6D[45]) to dissect the landscape of CRSC populations in human PCa. Finally, given that expression of specific CRSC markers is absent or highly heterogenous in subsets of patients, our study may suggest a gap in translating findings from basic science to translational research and clinical utility (ie, in experimental systems vs clinical specimens). It remains possible that identification of CRSC is model-dependent and/or that distinct CRSC populations characterize subgroups of PCa patients.

In summary, we provide a detailed analysis of the expression of known CRSC markers in the path toward castration-resistance and propose that CRSC-associated phenotypic clusters have clinical relevance. Our study paves the way toward a deeper elucidation of the relevance of CRSC markers in PCa progression and resistance to ADT.

## ACKNOWLEDGMENTS

The authors thank Petra Hirschmann and the IHC facility of the Institute of Pathology for assistance with the immunohistochemical analyses. Financial support was provided in part by the "Personenförderung" Program of the Department of Surgery at the University Hospital Basel (JFG), and by funding from the University of Basel (3MS1025, CL) and Fond'Action contre le cancer (CL). Components of some figures were created with BioRender.com.

## CONFLICT OF INTERESTS

The authors declare that there are no conflict of interests.

## ORCID

*Clémentine Le Magnen* http://orcid.org/0000-0002-6084-6054

## REFERENCES

1. Siegel RL, Miller KD, Jemal A. Cancer statistics, 2019. *CA Cancer J Clin*. 2019;69(1):7-34.
2. Ferlay J, Colombet M, Soerjomataram I, et al. Cancer incidence and mortality patterns in Europe: estimates for 40 countries and 25 major cancers in 2018. *Eur J Cancer*. 2018;103:356-387.
3. Attard G, Parker C, Eeles RA, et al. Prostate cancer. *Lancet*. 2016; 387(10013):70-82.

4. Clevers H. The cancer stem cell: premises, promises and challenges. *Nat Med*. 2011;17(3):313-319.
5. Zong Y, Goldstein AS. Adaptation or selection—mechanisms of castration-resistant prostate cancer. *Nat Rev Urol*. 2013;10(2):90-98.
6. Saygin C, Matei D, Majeti R, Reizes O, Lathia JD. Targeting Cancer Stemness in the Clinic: from hype to hope. *Cell Stem Cell*. 2019;24(1):25-40.
7. Ben-Porath I, Thomson MW, Carey VJ, et al. An embryonic stem cell-like gene expression signature in poorly differentiated aggressive human tumors. *Nat Genet*. 2008;40(5):499-507.
8. Smith BA, Balanis NG, Nanjundiah A, et al. A human adult stem cell signature marks aggressive variants across epithelial cancers. *Cell Rep*. 2018;24(12):e3355.
9. Le Magnen C, Shen MM, Abate-Shen C. Lineage plasticity in cancer progression and treatment. *Annu Rev Cancer Biol*. 2018;2:271-289.
10. Laudato S, Aparicio A, Giancotti FG. Clonal evolution and epithelial plasticity in the emergence of AR-independent prostate carcinoma. *Trends Cancer*. 2019;5(7):440-455.
11. Wang X, Kruithof-de Julio M, Economides KD, et al. A luminal epithelial stem cell that is a cell of origin for prostate cancer. *Nature*. 2009;461(7263):495-500.
12. Germann M, Wetterwald A, Guzmán-Ramirez N, et al. Stem-like cells with luminal progenitor phenotype survive castration in human prostate cancer. *Stem Cells*. 2012;30(6):1076-1086.
13. Yoo YA, Roh M, Naseem AF, et al. Bmi1 marks distinct castration-resistant luminal progenitor cells competent for prostate regeneration and tumour initiation. *Nat Commun*. 2016;7:12943.
14. Yoo YA, Vatapalli R, Lysy B, Mok H, Desouki MM, Abdulkadir SA. The role of castration-resistant Bmi1+Sox2+ cells in driving recurrence in prostate cancer. *J Natl Cancer Inst*. 2018;43:259.
15. Le Magnen C, Bubendorf L, Rentsch CA, et al. Characterization and clinical relevance of ALDHbright populations in prostate cancer. *Clinical Cancer Res*. 2013;19(19):5361-5371.
16. Gorodetska I, Lukiyanchuk V, Peitzsch C, Kozeretska I, Dubrovska ABRCA1. and EZH2 cooperate in regulation of prostate cancer stem cell phenotype. *Int J Cancer*. 2019;145:2974-2985.
17. Yan J, De Melo J, Cutz JC, Aziz T, Tang D. Aldehyde dehydrogenase 3A1 associates with prostate tumorigenesis. *Br J Cancer*. 2014;110(10):2593-2603.
18. Scher HI, Halabi S, Tannock I, et al. Design and end points of clinical trials for patients with progressive prostate cancer and castrate levels of testosterone: recommendations of the prostate cancer clinical trials working group. *J Clin Oncol*. 2008;26(7):1148-1159.
19. Kononen J, Bubendorf L, Kallioniemi A, et al. Tissue microarrays for high-throughput molecular profiling of tumor specimens. *Nat Med*. 1998;4(7):844-847.
20. Ruiz C, Holz DR, Oeggerli M, et al. Amplification and overexpression of vinculin are associated with increased tumour cell proliferation and progression in advanced prostate cancer. *J Pathol*. 2011;223(4):543-552.
21. Cerami E, Gao J, Dogrusoz U, et al. The cBio cancer genomics portal: an open platform for exploring multidimensional cancer genomics data. *Cancer Discov*. 2012;2(5):401-404.
22. Gao J, Aksoy BA, Dogrusoz U, et al. Integrative analysis of complex cancer genomics and clinical profiles using the cBioPortal. *Sci Signal*. 2013;6(269):pl1.
23. Cancer Genome Atlas Research N. The molecular taxonomy of primary prostate cancer. *Cell*. 2015;163(4):1011-1025.
24. Taylor BS, Schultz N, Hieronymus H, et al. Integrative genomic profiling of human prostate cancer. *Cancer Cell*. 2010;18(1):11-22.
25. Abida W, Cyrta J, Heller G, et al. Genomic correlates of clinical outcome in advanced prostate cancer. *Proc Natl Acad Sci USA*. 2019;116(23):11428-11436.
26. Robinson D, Van Allen EM, Wu YM, et al. Integrative clinical genomics of advanced prostate cancer. *Cell*. 2015;162(2):454.
27. Team RC. R: A language and environment for statistical computing. R Foundation for Statistical Computing, Vienna, Austria. URL http://www.R-project.org/. 2013.
28. van Buuren S, Groothuis-Oudshoorn K. mice: multivariate imputation by chained equations in R. *J Stat Softw*. 2011;45(3):1-67.
29. Gu Z, Eils R, Schlesner M. Complex heatmaps reveal patterns and correlations in multidimensional genomic data. *Bioinformatics*. 2016;32(18):2847-2849.
30. Therneau TM, Grambsch PM, Fleming T. https://www.semanticscholar.org/paper/A-Package-for-Survival-Analysis-in-S-Therneau-Grambsch/aba73f6957bce1648f066935f7ea85a99119be5d. 1994.
31. Kandoth C, McLellan MD, Vandin F, et al. Mutational landscape and significance across 12 major cancer types. *Nature*. 2013;502(7471):333-339.
32. Sotomayor P, Godoy A, Smith GJ, Huss WJ. Oct4A is expressed by a subpopulation of prostate neuroendocrine cells. *Prostate*. 2009;69(4):401-410.
33. Alexander RE, Cheng L, Grignon DJ, Idrees MT. Cytoplasmic OCT4 staining is a sensitive marker of neuroendocrine differentiation. *Hum Pathol*. 2014;45(1):27-32.
34. Pollack A, DeSilvio M, Khor LY, et al. Ki-67 staining is a strong predictor of distant metastasis and mortality for men with prostate cancer treated with radiotherapy plus androgen deprivation: radiation therapy oncology group trial 92-02. *J Clin Oncol*. 2004;22(11):2133-2140.
35. Fisher G, Yang ZH, Kudahetti S, et al. Prognostic value of Ki-67 for prostate cancer death in a conservatively managed cohort. *Br J Cancer*. 2013;108(2):271-277.
36. Conteduca V, Oromendia C, Eng KW, et al. Clinical features of neuroendocrine prostate cancer. *Eur J Cancer*. 2019;121:7-18.
37. Kweldam CF, Wildhagen MF, Steyerberg EW, Bangma CH, van der Kwast TH, van Leenders GJ. Cribriform growth is highly predictive for postoperative metastasis and disease-specific death in Gleason score 7 prostate cancer. *Mod Pathol*. 2015;28(3):457-464.
38. Dutta A, Le Magnen C, Mitrofanova A, Ouyang X, Califano A, Abate-Shen C. Identification of an NKX3.1-G9a-UTY transcriptional regulatory network that controls prostate differentiation. *Science*. 2016;352(6293):1576-1580.
39. van Schaijik B, Davis PF, Wickremesekera AC, Tan ST, Itinteang T. Subcellular localisation of the stem cell markers OCT4, SOX2, NANOG, KLF4 and c-MYC in cancer: a review. *J Clin Pathol*. 2018;71(1):88-91.
40. Vassalli G. Aldehyde dehydrogenases: not just markers, but functional regulators of stem cells. *Stem Cells Int*. 2019;2019:3904645.
41. Croker AK, Rodriguez-Torres M, Xia Y, et al. Differential functional roles of ALDH1A1 and ALDH1A3 in mediating metastatic behavior and therapy resistance of human breast cancer cells. *Int J Mol Sci*. 2017;18(10):2039.
42. Mu P, Zhang Z, Benelli M, et al. SOX2 promotes lineage plasticity and antiandrogen resistance in TP53- and RB1-deficient prostate cancer. *Science*. 2017;355(6320):84-88.
43. Villers A, McNeal JE, Freiha FS, Stamey TA. Multiple cancers in the prostate. Morphologic features of clinically recognized versus incidental tumors. *Cancer*. 1992;70(9):2313-2318.
44. Dirkse A, Golebiewska A, Buder T, et al. Stem cell-associated heterogeneity in Glioblastoma results from intrinsic tumor plasticity shaped by the microenvironment. *Nat Commun*. 2019;10(1):1787.

45. Barros-Silva JD, Linn DE, Steiner I, et al. Single-cell analysis identifies LY6D as a marker linking castration-resistant prostate luminal cells to prostate progenitors and cancer. *Cell Rep*. 2018;25(12):3504-3518.e6.

## SUPPORTING INFORMATION

Additional supporting information may be found online in the Supporting Information section.

**How to cite this article:** Federer-Gsponer JR, Müller DC, Zellweger T, et al. Patterns of stemness-associated markers in the development of castration-resistant prostate cancer. *The Prostate*. 2020;80:1108–1117. https://doi.org/10.1002/pros.24039